Composite spin liquid in a correlated topological insulator: Spin liquid without spin-charge separation

Jing He, Ying Liang, and Su-Peng Kou*

Department of Physics, Beijing Normal University, Beijing 100875, People's Republic of China

(Received 19 January 2012; revised manuscript received 29 March 2012; published 4 May 2012)

In this paper, we present an alternative type of insulator, namely composite spin liquid, which can be regarded as a short-range B-type topological spin-density wave as proposed by J. He *et al.* [Phys. Rev. B **84**, 035127 (2011)]. Composite spin liquid is a topological ordered state beyond the classification of traditional spin liquid states. The elementary excitations are the "composite electrons" with both spin and charge degrees of freedom, together with topological spin texture. This topological state supports the chiral edge mode but no topological degeneracy.

DOI: 10.1103/PhysRevB.85.205107 PACS number(s): 71.10.Pm, 75.10.Kt, 05.30.Pr

I. INTRODUCTION

The Fermi liquid based view of electronic properties has been very successful as a basis for understanding the physics of conventional solids including metals and (band) insulators. For band insulators, due to the energy gap, the charge degree of freedom is frozen. For magnetic insulators with spontaneous spin rotation symmetry breaking, the elementary excitations are gapped quasiparticles (an electron or a hole) that carry both spin and charge degrees of freedoms and the gapless spin wave (the Goldstone mode). For this case, the global symmetry is broken from SU(2) down to U(1). Thus the low-energy effective model is an O(3) nonlinear σ model (NLσM) that describes long-wavelength spin fluctuations.

However, in some special insulators with spin-rotation symmetry and translation symmetry, due to a big energy gap of the electrons, the charge degree of freedom is totally frozen, and there may be emergent gauge fields and deconfined spinons (elementary excitations with only the spin degree of freedom of an electron). These are referred to as *quantum spin liquids*.[1] Quantum spin liquid states have been pursued in spin models for more than two decades.[2–4] In certain spin models, the quantum spin liquids are accessed (in principle) by appropriate frustrating interactions. In general, there are three types of ansatz of spin liquid: SU(2), U(1), and Z_2.[3,4] The three different states may have the same global symmetry. This conflicts with Landau's theory, in which two states with the same symmetry belong to the same phase. Since one cannot use symmetry and order parameter to describe quantum orders, a new mathematical object—the projective symmetry group (PSG)—was introduced[3,4] to characterize the quantum order of spin liquid states.

Recently, there have been attempts to find spin liquids in the generalized Hubbard model of the intermediate coupling region, e.g., the Hubbard model on a triangular lattice, the Hubbard model on a honeycomb lattice, and the π-flux Hubbard model on a square lattice.[5–7] In addition, the quantum spin liquid state near the Mott transition (MI) of the Hubbard model on a honeycomb lattice has been confirmed by different approaches.[8–14] However, the nature of the spin liquid in the generalized Hubbard model of the intermediate coupling region is still a matter of debate.

We found that there may be another type of insulator with spin-rotation symmetry and translation symmetry, of which the elementary excitation has both spin and charge degrees of freedom. We call it *composite spin liquid*. Composite spin liquid (SL) can be regarded as short-range B-type topological spin-density wave (B-TSDW), which is beyond the classification of traditional spin liquid states. In a composite SL, there is no spin-charge separation: the elementary excitation is a so-called "composite electron"—a spin one-half charge $\pm e$ object trapping a topological spin texture (skyrmion or antiskyrmion). In addition, the composite SL is a topological spin liquid state with chiral edge states. However, similar to the case of the integer quantum Hall state, composite SL has no topological degeneracy for the ground state.

The paper is organized as follows. First, we write down the Hamiltonian of the topological Hubbard model. Secondly, we derive the effective O(3) nonlinear σ model with the Chern-Simons-Hopf (CSH) term to learn its properties. Next, chiral SL and composite SL are found to be the ground state of the short-range A-type topological spin-density wave and the short-range B-type topological spin-density wave, respectively. Finally, the conclusions are given. In addition, we compare composite SL with other exotic quantum states including fractional quantum Hall states, spin liquids, and topological insulators.

II. MODEL AND MEAN-FIELD RESULTS

The Hamiltonian of the topological Hubbard model on a honeycomb lattice is given by[15–17]

$$\begin{aligned} H = & -t \sum_{\langle i,j\rangle,\sigma} (\hat{c}^{\dagger}_{i\sigma}\hat{c}_{j\sigma} + \text{H.c.}) - t' \sum_{\langle\langle i,j\rangle\rangle,\sigma} e^{i\phi_{ij}} \hat{c}^{\dagger}_{i\sigma}\hat{c}_{j\sigma} \\ & - \mu \sum_{i,\sigma} \hat{c}^{\dagger}_{i\sigma}\hat{c}_{i\sigma} + U \sum_{i} \hat{n}_{i\uparrow}\hat{n}_{i\downarrow} \\ & + \varepsilon \sum_{i\in A,\sigma} \hat{c}^{\dagger}_{i\sigma}\hat{c}_{i\sigma} - \varepsilon \sum_{i\in B,\sigma} \hat{c}^{\dagger}_{i\sigma}\hat{c}_{i\sigma}. \end{aligned} \tag{1}$$

t and t' are the nearest-neighbor and next-nearest-neighbor hoppings, respectively. We introduce a complex phase ϕ_{ij} ($|\phi_{ij}| = \frac{\pi}{2}$) to the next-nearest-neighbor hopping, of which the positive phase is set to be clockwise. U is the on-site Coulomb repulsion. μ is the chemical potential and $\mu = U/2$ at half-filling. ε denotes an on-site staggered energy and is set to be $0.15t$.

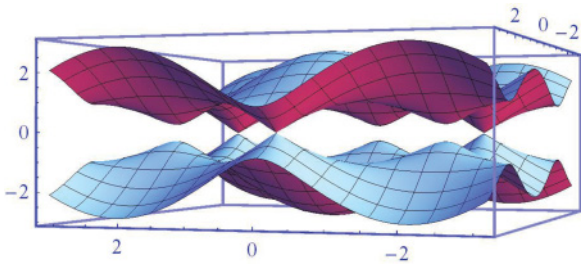

FIG. 1. (Color online) The dispersion of electrons for $t' = 0.0288t$ when $U = 0$. We can see clearly that at the high symmetry points, the energy gap is zero and the dispersions look like Dirac cones.

In the noninteracting limit ($U = 0$), the ground state is a $Q = 2$ topological insulator with a quantum anomalous Hall effect (QAH) for $t' > 0.0288t$ and a normal band insulator (BI) for $t' < 0.0288t$. At $t' = 0.0288t$, the electron energy gap closes at high symmetry points in momentum space. As a result, a third-order topological quantum phase transition occurs between a QAH and a BI. See the dispersion of electrons for $t' = 0.0288t$ in Fig. 1.

When we consider the on-site Coulomb interaction, the ground state can be an AF SDW order. We have calculated the mean-field value of staggered magnetization M that represents AF SDW order of the topological Hubbard model from the definition $\langle \hat{c}^{\dagger}_{i,\sigma} \hat{c}_{i,\sigma} \rangle = \frac{1}{2}[1 + (-1)^i \sigma M]$ in Ref. 15. Based on the mean-field results, the phase diagram has been obtained in Fig. 7 of Ref. 15. From the phase diagram we get five different quantum phases: two are nonmagnetic states with $M = 0$: the BI and the QAH; three are magnetic states with $M \neq 0$: the A-type topological AF SDW state (A-TSDW), the B-type topological AF SDW state (B-TSDW), and the trivial AF SDW state.

Let us explain the quantum phase transitions for different regions of t'. For $t' > 0.0288t$, the quantum phase transition between a QAH state and AF SDW order is always second order. Thus when we raise the interaction strength U, due to the smooth increase of the staggered magnetization, the QAH state will turn into the A-TSDW after crossing a magnetic phase transition, then into the B-TSDW crossing a topological quantum phase transition, and eventually into the trivial AF SDW state crossing another topological quantum phase transition. However, in the region of $t' < 0.0288t$, the quantum phase transition between a BI and AF SDW order is first order, which is denoted by the black line in Fig. 7 in Ref. 15. Due to the jumping of the staggered magnetization, the BI state will turn into B-TSDW directly and eventually turn into the trivial AF SDW state crossing a topological quantum phase transition. In the limit $t' \to 0$, the BI state will change into the trivial AF SDW state directly and there is no topological state at all. For the case of $t' = 0.0288t$, it is a semimetal for the weak-coupling limit ($U/t < 2.5$) without electron gap. When we raise the interaction strength U, due to the smooth increase of the staggered magnetization, the semimetal state will turn into the B-TSDW after crossing a second-order magnetic phase transition, and will eventually turn into the trivial AF SDW state crossing a topological quantum phase transition.

III. EFFECTIVE NLσM FOR MAGNETIC STATES

For the topological Hubbard model on a honeycomb lattice, there are three different magnetic states: A-TSDW, B-TSDW, and trivial AF SDW. A question here is whether these three SDWs with $M \neq 0$ are real long-range AF order. The nonzero value of M obtained by the mean-field method only indicates the existence of effective spin moments. It does not necessarily imply that the ground state is a long-range AF order because the direction of the spins is chosen to be fixed along the $\hat{\mathbf{z}}$ axis in the mean-field theory. Thus we will examine the stability of magnetic order against quantum spin fluctuations of effective spin moments based on a formulation by maintaining spin rotation symmetry, $\sigma_z \to \mathbf{\Omega} \cdot \boldsymbol{\sigma}$.

By replacing the electronic operators $\hat{c}^{\dagger}_i$ and $\hat{c}_j$ by Grassmann variables c^*_i and c_j, in the magnetic state we obtain the effective Lagrangian with spin rotation symmetry as

$$\begin{aligned}\mathcal{L}_{\text{eff}} = &\sum_{i,\sigma} c^*_{i\sigma} \partial_\tau c_{i\sigma} - t \sum_{\langle i,j\rangle,\sigma} (c^*_{i\sigma} c_{j\sigma} + \text{H.c.}) \\ &- t' \sum_{\langle\langle i,j\rangle\rangle,\sigma} e^{i\phi_{ij}} c^*_{i\sigma} c_{j\sigma} - \sum_i (-1)^i \Delta_M c^*_{i\sigma} \mathbf{\Omega}_i \cdot \boldsymbol{\sigma} c_{i\sigma} \\ &+ \varepsilon \sum_{i\in A,\sigma} c^*_{i\sigma} c_{i\sigma} - \varepsilon \sum_{i\in B,\sigma} c^*_{i\sigma} c_{i\sigma}, \end{aligned} \tag{2}$$

where $\Delta_M = UM/2$, Within Haldane's mapping, the spins are parametrized as $\mathbf{\Omega}_i = (-1)^i \mathbf{n}_i \sqrt{1 - \mathbf{L}_i^2} + \mathbf{L}_i$.[18–23] Here $\mathbf{n}_i$ is the Néel vector, $|\mathbf{n}_i| = 1$, and $\mathbf{L}_i$ is the transverse canting field, which is chosen to be $\mathbf{L}_i \cdot \mathbf{n}_i = \mathbf{0}$.

Then we integrate fermions and the transverse canting field and obtain the effective NLσM as

$$\mathcal{L}_{\mathbf{n}} = \frac{1}{2g}\left[\frac{1}{c}(\partial_\tau \mathbf{n})^2 + c(\nabla \cdot \mathbf{n})^2\right] \tag{3}$$

with a constraint $\mathbf{n}^2 = 1$. The coupling constant g and spin wave velocity c are defined as

$$g = \frac{c}{\rho_s}, \quad c^2 = \frac{\rho_s}{\chi^{\perp}}. \tag{4}$$

Here ρ_s is the spin stiffness and $\chi^{\perp}$ is the transverse spin susceptibility. The detailed calculations are given in Appendix A.

The properties of the effective NLσM are determined by the dimensionless coupling constant $\alpha = g\Lambda$. The cutoff is defined as $\Lambda = \min(1, \Delta E/c)$. Here ΔE is the energy gap of electrons. In particular, there is a critical point $\alpha_c = 4\pi$ (or $g_c = \frac{4\pi}{\Lambda}$). See the illustration in Fig. 2. The quantum critical point (QCP) separates the long-range spin order from the short-range spin order (the quantum disordered state). The dotted line shows the renormalized spin stiffness of the long-range spin order and the energy scale of the spin gap of the quantum disordered state, respectively (see the discussion below).

For the case of $\alpha < 4\pi$, we obtain solutions of the spin condensed n_0 and the spin gap m_s at zero temperature:

$$n_0 = \left(1 - \frac{g}{g_c}\right)^{1/2}, \quad m_s = 0. \tag{5}$$

At finite temperature, the solutions become $n_0 = 0$ and $m_s = 2k_B T \sinh^{-1}[e^{-\frac{2\pi c}{gk_B T}} \sinh(\frac{c\Lambda}{2k_B T})]$. Because the energy scale of

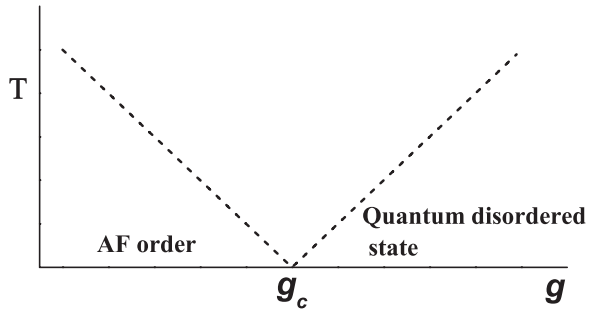

FIG. 2. The illustration of the relationship between AF order and the quantum disordered state.

the spin gap m_s is always much smaller than the temperature, i.e., $m_s \ll k_B T$ (or ω_n), quantum fluctuations become negligible in a sufficiently long-wavelength and low-energy regime ($m_s < |c\mathbf{q}| < k_B T$). Thus in this region one may only consider the purely static (semiclassical) fluctuations. The effective Lagrangian of the NLσM then becomes

$$\mathcal{L} = \frac{\rho_{s,\mathrm{eff}}}{2}(\nabla \cdot \mathbf{n})^2, \tag{6}$$

where $\rho_{s,\mathrm{eff}} = c(\frac{1}{g} - \frac{1}{g_c})$ is the renormalized spin stiffness. At zero temperature, the mass gap vanishes, which means that long-range AF order appears. To describe the long-range AF order, we introduce a spin order parameter,

$$\mathcal{M}_0 = \frac{M}{2} n_0 = \frac{M}{2}\left(1 - \frac{g}{g_c}\right)^{1/2}, \quad m_s = 0. \tag{7}$$

The ground state of the long-range AF ordered phase has a finite spin order parameter, and in this region there are two transverse Goldstone modes (between them the interaction is irrelevant).

For the case of $\alpha > 4\pi$, the interaction between Goldstone modes becomes relevant and at low energy the renormalized coupling constant diverges. Consequently, the spin gap opens and the long-range spin order disappears, which mean that the ground state may be a quantum disordered state, and we obtain the effective model of massive spin-1 excitations,

$$\mathcal{L}_\mathbf{s} = \frac{1}{2g}\left[(\partial_\mu \mathbf{n})^2 + m_s^2 \mathbf{n}^2\right], \tag{8}$$

with the solutions of n_0 and m_s as

$$n_0 = 0, m_s = 4\pi c\left(\frac{1}{g_c} - \frac{1}{g}\right). \tag{9}$$

Using the CP(1) representation, we have

$$\mathcal{L}_\mathbf{s} = \frac{2}{g}\left[|(\partial_\mu - i a_\mu)\mathbf{z}|^2 + m_z^2 \mathbf{z}^2\right], \tag{10}$$

where $\mathbf{z}$ is a bosonic spinon, $\mathbf{z} = (z_1, z_2)^T$, $\mathbf{n}_i = \bar{\mathbf{z}}_i \boldsymbol{\sigma} z_i$, $\bar{\mathbf{z}}\mathbf{z} = \mathbf{1}$, and $a_\mu \equiv -\frac{i}{2}(\bar{\mathbf{z}}\partial_\mu \mathbf{z} - \partial_\mu \bar{\mathbf{z}}\mathbf{z})$. Here a_μ is introduced as an assistant gauge field. Specifically, the local gauge transformation is $z \to e^{i\varphi(r,\tau)} z$. m_z denotes the mass gap for spinons as $m_z = m_s/2$.

In addition, after integrating over fermions by using the gradient expansion approach, we also obtain the Chern-Simons-Hopf (CSH) term as[15,24]

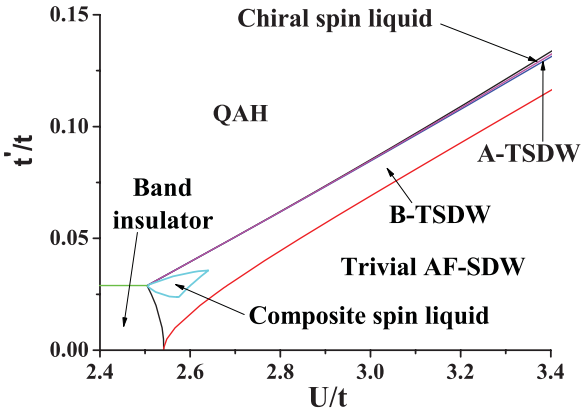

FIG. 3. (Color online) The phase diagram. There are seven phases: QAH, band insulator, A-TSDW, B-TSDW, chiral spin liquid, composite spin liquid, and trivial AF-SDW. The regions of chiral spin liquid and composite spin liquid are the quantum disordered regions of $\alpha > 4\pi$.

$$\mathcal{L}_{\mathrm{CSH}} = -i \sum_{I,J} \frac{\mathcal{K}_{IJ}}{4\pi} \varepsilon^{\mu\nu\lambda} a_\mu^I \partial_\nu a_\lambda^J, \tag{11}$$

where $\mathcal{K}$ is a 2×2 matrix, $a_\mu^{I=1} = A_\mu$, and $a_\mu^{I=2} = a_\mu$. A_μ is the electric-magnetic field. The "charges" of A_μ and a_μ are defined by q and q_s, respectively. Thus for different SDW orders with the same order parameter M, we have different $\mathcal{K}$ matrices : for A-TSDW order, $\mathcal{K} = \left(\begin{smallmatrix} 2 & 0 \\ 0 & 2 \end{smallmatrix}\right)$; for B -TSDW order, $\mathcal{K} = \left(\begin{smallmatrix} 1 & 1 \\ 1 & 1 \end{smallmatrix}\right)$; for trivial SDW order, $\mathcal{K} = 0$. See detailed calculations in Appendix B.

For different regions of t', we calculated the dimensionless coupling constant g (α) and derived the quantum phase transitions between long-range and short-range AF SDW order. Thus we can plot a new phase diagram in Fig. 3 that shows the quantum disordered regions of $\alpha > 4\pi$ (the regions of chiral spin liquid and composite spin liquid).

For a given t' bigger than $0.0288t$, there are two situations. Figure 4 shows the dimensionless coupling constant for one situation with the parameter $t' = 0.1t$. In Fig. 4 there is a quantum disordered region with $\alpha > \alpha_c = 4\pi$ in A-TSDW that corresponds to the chiral spin liquid (yellow region). The other case is shown in Fig. 5, of which the dimensionless

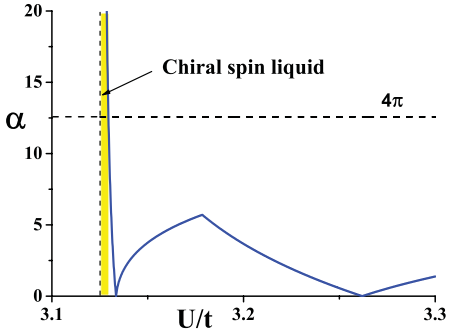

FIG. 4. (Color online) The dimensionless coupling constant $\alpha = g\Lambda$ for the case of the parameter as $t' = 0.1t$. For the region with $\alpha > 4\pi$, the ground state is chiral spin liquid (yellow region).

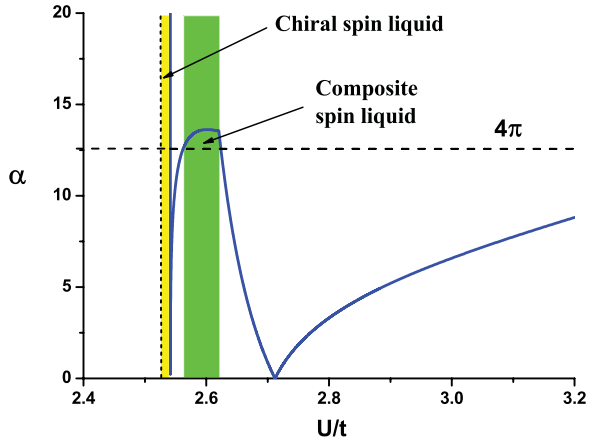

FIG. 5. (Color online) The dimensionless coupling constant $\alpha = g\Lambda$ for the case of the parameter as $t' = 0.033t$. For the regions with $\alpha > 4\pi$, the ground states are spin liquid states—chiral spin liquid (yellow region) or composite spin liquid (green region).

coupling constant for the parameter $t' = 0.033t$. There are two quantum disordered regions with $\alpha > \alpha_c = 4\pi$: one corresponds to the chiral spin liquid (yellow region) in A-TSDW, the other is composite spin liquid (green region) in B-TSDW (see the discussion in the following sections). For this case, we get the energy gap of spin order parameter $\mathcal{M}_0$ and spin excitations m_s in Figs. 6 and 7. One can see that in chiral spin liquid and composite spin liquid, $\mathcal{M}_0 = 0$ and $m_s \neq 0$. For the case of $t' = 0.0288t$, we show the result of the dimensionless coupling constant in Fig. 8, from which one can see that there is a quantum disordered region with $\alpha > \alpha_c = 4\pi$ in B-TSDW that corresponds to the composite spin liquid (green region). For this case, we also get the spin order parameter $\mathcal{M}_0$ and the energy gap of spin excitations m_s in Figs. 9 and 10. One can see that in composite spin liquid, $\mathcal{M}_0 = 0$ and $m_s \neq 0$. For a given t' smaller than $0.0288t$, there are also two situations. For $0.023\,77t < t' < 0.0288t$, from the result shown in Fig. 11 ($t' = 0.025t$), we found a quantum disordered region with $\alpha > \alpha_c = 4\pi$ in B-TSDW that corresponds to the composite spin liquid (green region). For

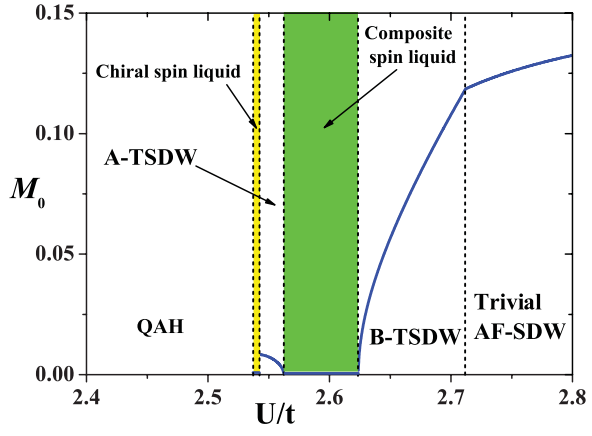

FIG. 6. (Color online) The spin order parameter $\mathcal{M}_0$ for the case of the parameter as $t' = 0.033t$. Yellow region denotes chiral spin liquid and green region denotes composite spin liquid, of which $\mathcal{M}_0 = 0$.

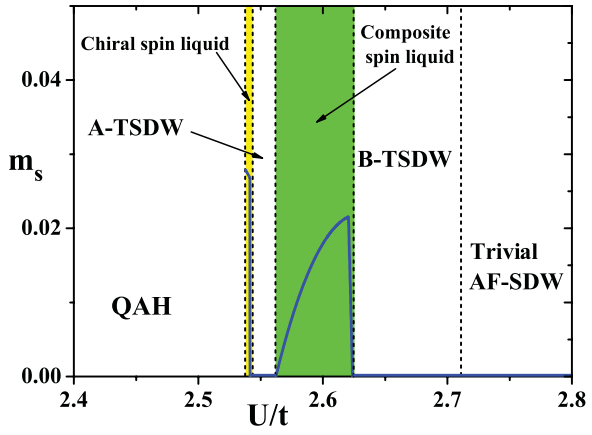

FIG. 7. (Color online) The spin gap m_s for the case of the parameter as $t' = 0.033t$. Yellow region denotes chiral spin liquid and green region denotes composite spin liquid, of which $m_s \neq 0$.

$0 < t' < 0.023\,77t$, we found that the dimensionless coupling constant α is always smaller than $\alpha_c = 4\pi$. That means there is no quantum disordered region at all. We also plot Fig. 12 to show this situation ($t' = 0.02t$).[25]

In the following sections, we will use the effective model with CSH terms to learn the properties of different SDW orders:[15]

$$\mathcal{L}_{\text{eff}} = \mathcal{L}_{\text{s}} + \mathcal{L}_{\text{CSH}},$$

where

$$\mathcal{L}_{\text{s}} = \frac{1}{2g}\left[(\partial_\mu \mathbf{n})^2 + m_s^2 \mathbf{n}^2\right]$$

and

$$\mathcal{L}_{\text{CSH}} = \sum_{I,J} \frac{K_{IJ}}{4\pi} \varepsilon^{\mu\nu\lambda} a_\mu^I \partial_\nu a_\lambda^J.$$

Thus an important issue is determining the *nature* of these quantum disordered states with different CSH terms. Our answer is as follows: for the case of A-TSDW with $\mathcal{K} = \left(\begin{smallmatrix} 2 & 0 \\ 0 & 2 \end{smallmatrix}\right)$, the quantum disordered state is a chiral spin liquid with topological degeneracy and anyonic excitations (see the

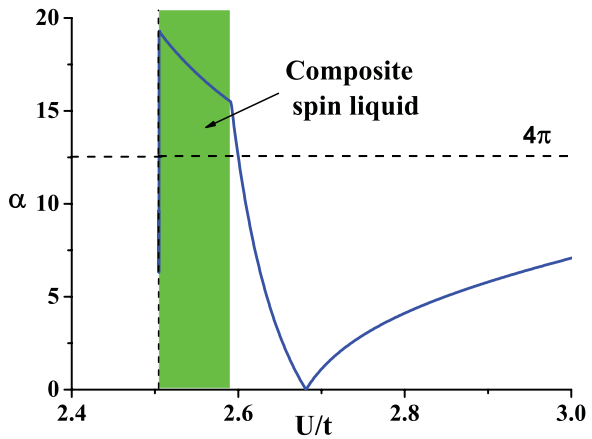

FIG. 8. (Color online) The dimensionless coupling constant $\alpha = g\Lambda$ for the case of the parameter as $t' = 0.0288t$. For the region with $\alpha > 4\pi$, the ground state is composite spin liquid (green region).

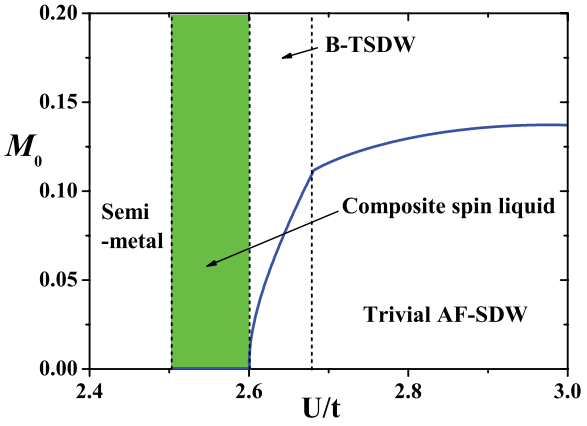

FIG. 9. (Color online) The spin order parameter $\mathcal{M}_0$ for the case of the parameter as $t' = 0.0288t$. The green region denotes composite spin liquid, of which $\mathcal{M}_0 = 0$.

illustration in Fig. 13); for the case of B-TSDW with $\mathcal{K} = \left(\begin{smallmatrix} 1 & 1 \\ 1 & 1 \end{smallmatrix}\right)$, the quantum disordered state is composite spin liquid with chiral edge states, of which the elementary excitation is spin one-half charge $\pm e$ objects trapping a topological spin texture (see the illustration in Fig. 15).

IV. CHIRAL SPIN LIQUID–QUANTUM DISORDERED STATE OF A-TSDW

First, we study the quantum disordered state of A-TSDW that is described by

$$\mathcal{L}_{\text{eff}} = \frac{1}{2g}\left[(\partial_\mu \mathbf{n})^2 + m_s^2 \mathbf{n}^2\right] + \frac{1}{2\pi}\epsilon^{\mu\nu\lambda} A_\mu \partial_\nu A_\lambda + \frac{1}{2\pi}\epsilon^{\mu\nu\lambda} a_\mu \partial_\nu a_\lambda$$

or

$$\mathcal{L}_{\text{eff}} = \frac{2}{g}\left[|(\partial_\mu - i a_\mu)\mathbf{z}|^2 + m_z^2 \mathbf{z}^2\right] + \frac{1}{2\pi}\epsilon^{\mu\nu\lambda} A_\mu \partial_\nu A_\lambda + \frac{1}{2\pi}\epsilon^{\mu\nu\lambda} a_\mu \partial_\nu a_\lambda. \quad (12)$$

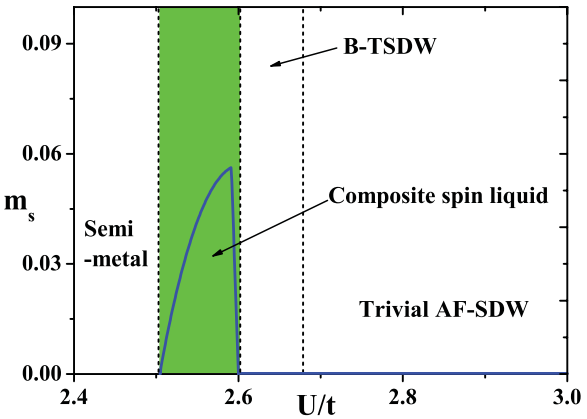

FIG. 10. (Color online) The spin gap m_s for the case of the parameter as $t' = 0.0288t$. The green region denotes composite spin liquid, of which $m_s \neq 0$.

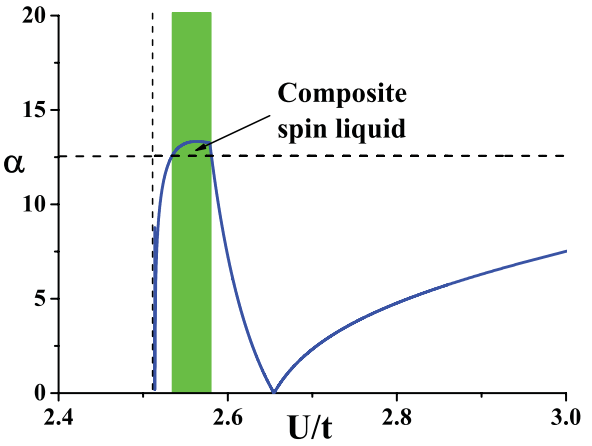

FIG. 11. (Color online) The dimensionless coupling constant $\alpha = g\Lambda$ for the case of the parameter as $t' = 0.025t$. For the region with $\alpha > 4\pi$, the ground state is composite spin liquid (green region).

At the low-energy limit, the kinetic term of gauge field a_μ is induced,

$$\mathcal{L}(a_\mu) = \frac{1}{4e_a^2}(\partial_\mu a_\nu)^2. \quad (13)$$

The induced coupling constant of the three-dimensional gauge field is $e_a^2 = 3\pi m_z^2$. After considering the CSH term, we obtain the effective Lagrangian as

$$\mathcal{L}_{\text{eff}} = \frac{1}{4e_a^2}(\partial_\mu a_\nu)^2 + \frac{1}{2\pi}\epsilon^{\mu\nu\lambda} a_\mu \partial_\nu a_\lambda + \frac{1}{2\pi}\epsilon^{\mu\nu\lambda} A_\mu \partial_\nu A_\lambda. \quad (14)$$

For the compact U(1) gauge theory in $2+1$ dimensions, there are instantons (space-time "magnetic" monopoles) that generate 2π gauge flux of a_μ, which indicates that the a_μ gauge field is "compact."[26] Without the CSH term, the monopoles form Coulomb gas in $2+1$ dimensions. Due to the Debye screening in the monopole plasma, the gauge field a_μ obtains a mass gap, and bosonic spinons $\mathbf{z}$ that couple the gauge field a_μ are confined. It is pointed out in Ref. 27 that from the

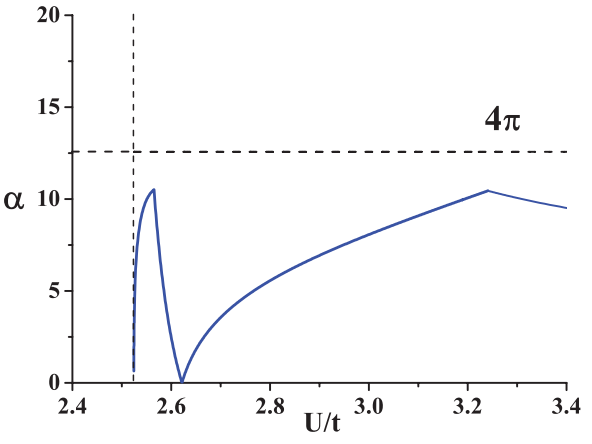

FIG. 12. (Color online) The dimensionless coupling constant $\alpha = g\Lambda$ for the case of the parameter as $t' = 0.02t$. We can see that the dimensionless coupling constant α is always smaller than $\alpha_c = 4\pi$. That mean there does not exist a quantum disordered region at all.

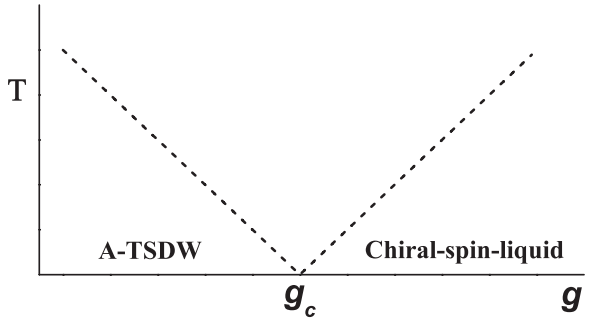

FIG. 13. The illustration of the relationship between A-TSDW and chiral spin liquid.

Berry phase of a path integral of a spin coherent state on a honeycomb lattice, the ground state with spinon confinement is really a VBS state with spontaneous translation symmetry breaking.

However, due to the Chern-Simon term, $\frac{1}{2\pi}\epsilon^{\mu\nu\lambda}a_\mu\partial_\nu a_\lambda$, the instantons are confined by linear potential and are irrelevant to low-energy physics. Thus the ground state cannot be a VBS state and spinons are deconfined. In particular, the Chern-Simons term for a_μ has a nontrivial statistics effect. Because the low-energy physics is dominated only by spinon $\mathbf{z}$, due to $\frac{1}{2\pi}\epsilon^{\mu\nu\lambda}a_\mu\partial_\nu a_\lambda$, the statistics angle of $\mathbf{z}$ is $\pi/2$. As a result, spinon $\mathbf{z}$ becomes a semi-ionic particle with spin $J=\frac{1}{4}$. Therefore, the quantum disordered state of A-TSDW that is described by the effective Lagrangian in Eq. (12) is really a topological ordered state, i.e., chiral spin liquid. From the CSH term, one may derive topological degeneracy—two degenerate ground states of chiral spin liquid on a torus.[28] The result is consistent with that in Ref. 17.

In addition, one can also derive the edge states from the effective CSH theory. There are two right-moving "spin" edge excitations described by the following one-dimensional (1D) fermion theory:[29]

$$\mathcal{L}_{\text{edge}}=\sum_\alpha \psi^\dagger_{\alpha s}(\partial_t - v_R\partial_x)\psi_{\alpha s},$$

where $\alpha=1,2$. $\psi_{\alpha s}$ carries a unit of a_μ charge. One can see "spin" chiral edge states in Fig. 14 (the lines with arrows). Correspondingly, one can obtain the quantized spin Hall conductivity,

$$\sigma_s=\lim_{\omega\to 0}\frac{1}{\omega}\epsilon_{ij}\langle J_{si}(\omega,0)J_{sj}(-\omega,0)\rangle=\frac{2e^2}{h}. \tag{15}$$

Here J_{si} denotes spin current, $J_{si}=-i\langle\sum_a \bar\psi_a\gamma_i\mathbf{n}\cdot\sigma\psi_a\rangle$.

On the other hand, we discuss the properties of A_μ. The gauge field A_μ is a classical field and has no dynamic terms. Thus the Chern-Simons term for A_μ only indicates the quantized anomalous charge Hall effect. From it, we find two right-moving branches of "charge" edge excitations, which are described by the following 1D fermion theory:[30]

$$\mathcal{L}_{\text{edge}}=\sum_\alpha \psi^\dagger_{c,\alpha}(\partial_t - v_c\partial_x)\psi_{c,\alpha}, \tag{16}$$

where $\alpha,\beta=1,2$. $\psi_{c,\alpha}$ carries a unit of A_μ charge. One can see a "charge" chiral edge state (the lines with dots) in Fig. 14. Consequently, we get the quantized charge Hall conductivity $\sigma_H=\frac{2e^2}{h}$.

Finally, we identify the quantum disordered state of A-TSDW characterized by $g>g_c$ as a chiral spin liquid with the quantum anomalous Hall effect (see the illustration in Fig. 13). For this system, there is spin-charge separation. In Fig. 13, the QCP at $g=g_c$ denotes the quantum phase transition dividing long-range A-TSDW and short-range A-TSDW (chiral SL). In addition, we should emphasize the existence of the chiral spin liquid due to strongly fluctuated spin moments characterized by the divergent behavior of the spin coupling constant near the quantum phase transition (yellow region) in Figs. 4 and 5 as $g\to g_c$. Thus the existence of the chiral spin liquid is independent of the cutoff Λ.

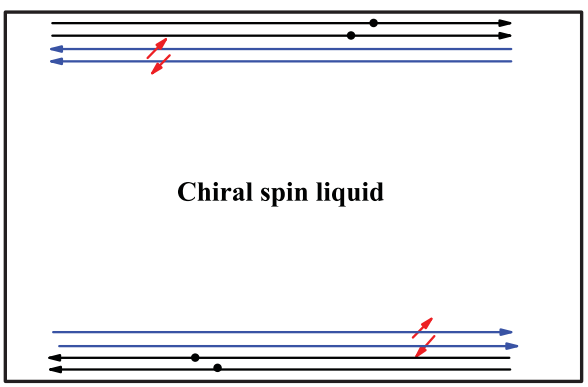

FIG. 14. (Color online) The illustration of the edge state of chiral spin liquid. There exists a "spin" chiral edge state (the lines with arrows) and a "charge" chiral edge state (the lines with dots).

V. COMPOSITE SPIN LIQUID–QUANTUM DISORDERED STATE OF B-TSDW

Next we study the quantum disordered state of B-TSDW that is described by the low-energy effective Lagrangian

$$\mathcal{L}_{\text{eff}}=\frac{1}{2g}\left[(\partial_\mu\mathbf{n})^2+m_s^2\mathbf{n}^2\right]+\frac{1}{4\pi}\epsilon^{\mu\nu\lambda}A_\mu\partial_\nu A_\lambda + \frac{1}{2\pi}\epsilon^{\mu\nu\lambda}A_\mu\partial_\nu a_\lambda+\frac{1}{4\pi}\epsilon^{\mu\nu\lambda}a_\mu\partial_\nu a_\lambda$$

or

$$\mathcal{L}_{\text{eff}}=\frac{2}{g}\left[|(\partial_\mu - ia_\mu)\mathbf{z}|^2+m_z^2\mathbf{z}^2\right]+\frac{1}{2\pi}\epsilon^{\mu\nu\lambda}A_\mu\partial_\nu a_\lambda + \frac{1}{4\pi}\epsilon^{\mu\nu\lambda}A_\mu\partial_\nu A_\lambda+\frac{1}{4\pi}\epsilon^{\mu\nu\lambda}a_\mu\partial_\nu a_\lambda.$$

From Fig. 15, one can find that there is indeed a region of short-range B-TSDW order that is characterized by $g>g_c$.

First, we study the statistics of spinon $\mathbf{z}$. To learn the statistics of spinon $\mathbf{z}$, we can set A_μ to be zero because A_μ is a classical field. Thus the CS term is reduced to $\frac{1}{4\pi}\epsilon^{\mu\nu\lambda}a_\mu\partial_\nu a_\lambda$. We can see that the spinons are fermionic particles by binding a 2π flux of a_μ that is just a skyrmion (or an antiskyrmion). On the other hand, due to the mutual Chern-Simons term $\frac{1}{2\pi}\epsilon^{\mu\nu\lambda}A_\mu\partial_\nu a_\lambda$, a 2π flux of a_μ will carry an electric charge. Thus the $\mathbf{z}$ particle is really an "electron" or a "hole" binding a skyrmion (or antiskyrmion). In the following, we will call such a composite object a "composite electron (hole)."

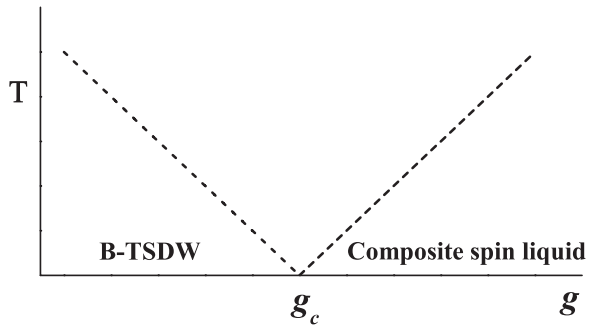

FIG. 15. The illustration of the relationship between B-TSDW and composite spin liquid.

Due to the Chern-Simon term $\frac{1}{4\pi}\epsilon^{\mu\nu\lambda}a_\mu\partial_\nu a_\lambda$, the instantons are also confined by linear potential and are irrelevant to low-energy physics. Thus the spinons are also deconfined. Figure 16 shows the mass gap of the **z** particle for the parameter $t' = 0.033t$, $2m_z = 4\pi c(\frac{1}{g_c} - \frac{1}{g})$. One can see that m_z is always much smaller than the mass gap of electrons, ΔE, as $m_z \ll \Delta E$. So the low-energy physics is dominated by the **z** particle, the so-called composite electron (hole).

Secondly, we study the properties of gauge fluctuations. After integrating the massive **z** particle, the effective Lagrangian for gauge field a_μ becomes

$$\mathcal{L}_{\text{eff}} = \frac{1}{4e_a^2}(\partial_\mu a_\nu)^2 + \frac{1}{4\pi}\epsilon^{\mu\nu\lambda}a_\mu\partial_\nu a_\lambda + \frac{1}{2\pi}\epsilon^{\mu\nu\lambda}A_\mu\partial_\nu a_\lambda + \frac{1}{4\pi}\epsilon^{\mu\nu\lambda}A_\mu\partial_\nu A_\lambda. \quad (17)$$

Then the partition function of the effective model is written as

$$\mathcal{Z} = \int \mathcal{D}[a]e^{-\int_0^\beta d\tau\mathcal{L}_{\text{eff}}}.$$

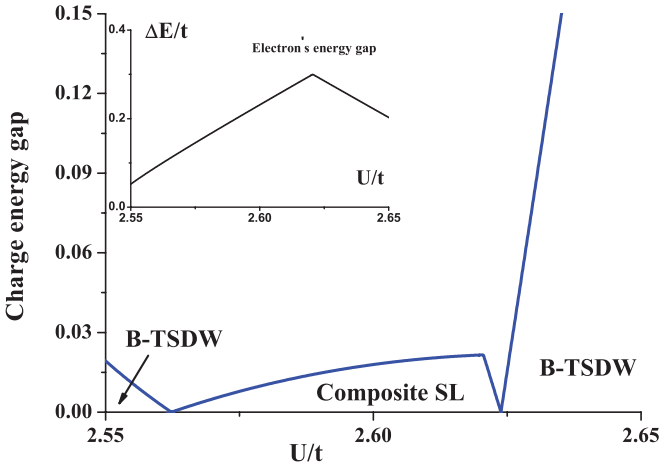

FIG. 16. (Color online) The charge energy gap for the case of $t' = 0.033t$, $\varepsilon = 0.15t$: the charge carrier is a composite electron. In composite SL, the charge energy gap is that of spin gap, m_s; in B-TSDW, the charge energy gap is that of a skyrmion and an antiskyrmion, Δ_c. The energy gap of fermion quasiparticles is very big (see inset).

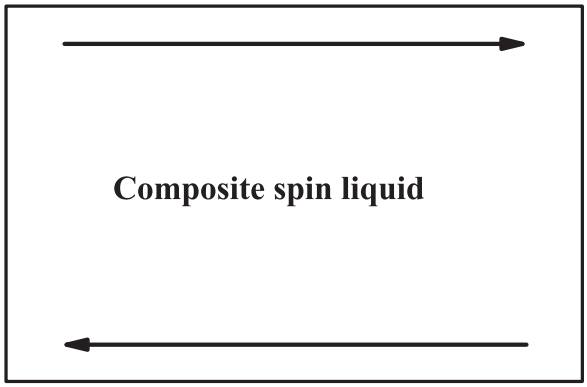

FIG. 17. The illustration of the edge state of composite spin liquid. There exists a single chiral edge mode.

We introduce $a_{+,\mu} = A_\mu + a_\mu$, $a_{-,\mu} = A_\mu - a_\mu$, and obtain the partition function as

$$\mathcal{Z} = \int \mathcal{D}[a_+]e^{-\int_0^\beta d\tau\mathcal{L}_{\text{eff}}},$$

where

$$\mathcal{L}_{\text{eff}} = \frac{1}{4e_a^2}(\partial_\mu a_{\nu,+})^2 + \frac{1}{4\pi}\epsilon^{\mu\nu\lambda}a_{\mu,+}\partial_\nu a_{\lambda,+}. \quad (18)$$

With the Chern-Simons term $\frac{1}{4\pi}\epsilon^{\mu\nu\lambda}a_{\mu,+}\partial_\nu a_{\lambda,+}$, the gauge field $a_{\mu,+}$ indicates quantized spin-charge synchronized edge states and the quantized spin-charge synchronized Hall effect pointed out in Ref. 1. The edge excitation is described by the following one-dimensional fermion theory:[29,30]

$$\mathcal{L}_{\text{edge}} = \tilde{\psi}^\dagger(\partial_t - \tilde{v}\partial_x)\tilde{\psi}, \quad (19)$$

where $\tilde{\psi}$ carries a unit of $a_{+,\mu}$ "charge." One can see a chiral edge mode (the lines in Fig. 17). Consequently, we get the spin-charge synchronized Hall conductivity as

$$\tilde{\sigma} = \lim_{\omega\to 0}\frac{1}{\omega}\epsilon_{ij}\langle\tilde{J}_i(\omega,0)\tilde{J}_j(-\omega,0)\rangle = \frac{e^2}{h}, \quad (20)$$

where

$$\tilde{J}_i = i\left\langle\sum_a \bar{\psi}_a\gamma_i(1-\mathbf{n}\cdot\sigma)\psi_a/2\right\rangle. \quad (21)$$

Finally, we use the duality relationship between spinons and skyrmions to learn the quantum phase transition at $g = g_c$ dividing long-range B-TSDW and short-range B-TSDW (composite SL).

In B-TSDW, we can define the skyrmion (or antiskyrmion) with winding number $\mathcal{Q} = \int \mathbf{d^2r}\frac{1}{4\pi}\epsilon_{0\nu\lambda}\mathbf{n}_s\cdot\partial^\nu\mathbf{n}_s\times\partial^\lambda\mathbf{n}_s = \pm 1$, of which the solutions in the continuum limit are[31]

$$\mathbf{n}_s = \left(\frac{\lambda(x-x_0)}{|\mathbf{r}-\mathbf{r}_0|^2+\lambda^2}, \pm\frac{\lambda(y-y_0)}{|\mathbf{r}-\mathbf{r}_0|^2+\lambda^2}, \pm\frac{\lambda}{|\mathbf{r}-\mathbf{r}_0|^2+\lambda^2}\right). \quad (22)$$

Here λ is the radius of the skyrmion at $\mathbf{r}_0 = (x_0, y_0)$. In long-range B-TSDW, due to the "spin-charge synchronized charge-flux binding" effect, the $Q = \pm 1$ skyrmion carries a unit electric charge $q = \mp 1$ and a unit "charge" $q_s = \mp 1$.

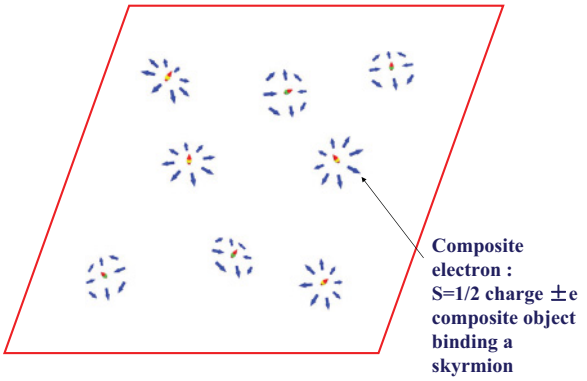

FIG. 18. (Color online) The illustration of composite spin liquid, of which the elementary excitations are the "composite electrons" that are $S = 1/2$ charge $\pm e$ fermions with trapping a topological spin texture.

With a unit "charge" q_s, a $Q = \pm 1$ skyrmion gets half spin and becomes a charged $S = 1/2$ fermion.

The mass of the skyrmion (or antiskyrmion) is associated with

$$m_{\text{skyrmion}} = m_{\text{antiskyrmion}} = \frac{\rho_{s,\text{eff}}}{2} \int d^2\mathbf{r}(\nabla \cdot \mathbf{n}_s)^2 = 4\pi\rho_{s,\text{eff}},$$

where $\rho_{s,\text{eff}} = (1 - \frac{g}{g_c})\rho_s$. This result indicates the charge gap is really the mass gap of a skyrmion-antiskyrmion pair,

$$\Delta_c = m_{\text{skyrmion}} + m_{\text{antiskyrmion}} = 8\pi\left(1 - \frac{g}{g_c}\right)\rho_s, \quad (23)$$

that will close at the critical point $g = g_c$, $\Delta_c \to 0$. From Fig. 5, one can see that there are two QCPs ($g = g_c$) between B-TSDW and composite SL where the charged excitations have no energy gap, while the usual electrons without a trapping spin texture still have a big mass gap $\Delta E \gg \Delta_c$ (see the inset of Fig. 16). In B-TSDW, the low-energy charge dynamics is dominated by fermionic charged skyrmions rather than the electrons. At these QCPs, the system is a semimetal with gapless charge excitations. The dotted line in Fig. 15 is the energy scale of the charge gap.

Finally, we find that there is a new type of spin liquid–composite spin liquid. The low-energy excitations are "composite electrons" that are $S = 1/2$ charge $\pm e$ fermions trapping a topological spin texture. See the illustration in Fig. 18. At the QCPs between long-range B-TSDW and composite SL, the system becomes a semimetal with gapless charge excitations (even for gapped electrons).

VI. CONCLUSION AND DISCUSSION

We presented an alternative type of topological state that we refer to as "composite spin liquid." A composite spin liquid state can be regarded as a short-range B-type topological spin-density wave that is beyond the classification of traditional spin liquid states. For traditional spin liquid states there always exists spin-charge separation, while for composite spin liquid there is no spin-charge separation. Instead, the elementary excitations are "composite electrons" with both spin and charge degrees of freedom, together with topological spin texture. This topological state supports a single chiral edge mode but no topological degeneracy. In addition, the QCPs between long-range B-TSDW and composite SL are also nontrivial, therefore the system becomes a semimetal with gapless charge excitations (even for gapped electrons).

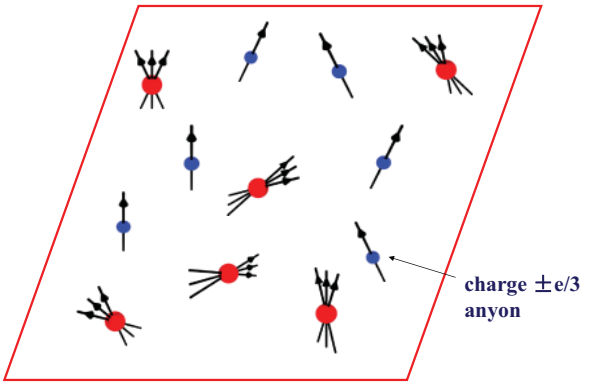

FIG. 19. (Color online) The illustration of the fractional quantum Hall state. Small blue balls with single arrows denote the anyonic excitations with $\pm e/3$ charge.

In addition, we compare different exotic quantum orders beyond Landau's theory:

(i) *Fractional quantum Hall (FQH) state*. Due to the charge-flux binding effect, the elementary excitations are anyonic excitations with fractional electric charge and fractional quantized Hall conductivity.[33,34] Figure 19 shows anyonic excitations with $\pm e/3$ charge (small blue balls with a single arrow). The ground state on a torus has topological degeneracy. For the open system, there are chiral edge states on its boundary. Fractional quantized Hall states can be classified into different Abelian states and non-Abelian states using effective CS theories (or K-matrix theory[24,35,36]).

(ii) *Topological band insulator (TBI)*. The elementary excitations are gapped electrons (or holes). For this topological state, there exist gapless edge states. However, there is no topological degeneracy for the ground state. Topological band insulators can be classified into Z_2 type or Z type using the "tenfold" random matrix.[37–39]

(iii) *Spin liquid (SL)*. Due to the big electron gap (Mott gap), the excitations are deconfined spinons with only a spin degree of freedom. In Fig. 20, the blue arrow denotes an $S = 1/2$ chargeless spinon. Quantum spin liquid states can be

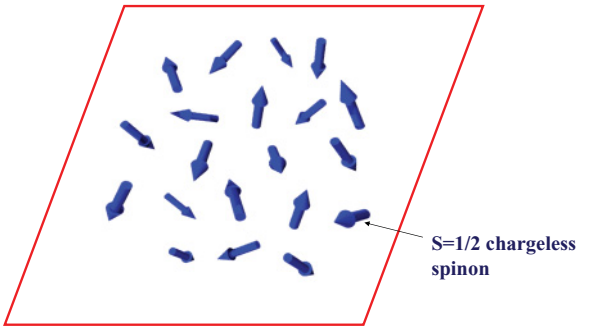

FIG. 20. (Color online) The illustration of quantum spin liquid. The blue arrows denote an $S = 1/2$ chargeless spinon.

TABLE I. The differences (the types of excitations, if there exists topological degeneracy for the ground states on the torus, if there exist edge states, and the way to classify the topological states) between four exotic quantum orders beyond Landau's theory: the fractional quantum Hall state (FQH), a topological band insulator (TBI), spin liquid (SL), and composite spin liquid (SL).

	Excitations	Topological degeneracy	Edge state	Classification
FQH state	Charged anyon	Yes	Yes	K matrix
TBI	Electron	No	Yes	Tenfold way
SL	Spinon	–	–	PSG
Composite SL	Composite electron	No	Yes	?

classified into SU(2) type, U(1) type, or Z_2 type using PSGs.[3,4] For topological spin liquid (for example, chiral spin liquid) there exist gapless edge states and topological degeneracy, while for gapless spin liquid (for example, algebraic spin liquid) there are no well-defined gapless edge states and topological degeneracy. For this reason, we use "–" to denote the uncertainty in Table I.

(iv) *Composite spin liquid*. The elementary excitations are the "composite electrons" with both spin and charge degrees of freedom, together with topological spin texture (see Fig. 18). For this topological states, there exist gapless edge states but no topological degeneracy. As of yet, we do not know how to characterize composite spin liquid states. For this reason, we use "?" to denote the situation in Table I.

Finally, we address the relevant experimental realization. This topological Hubbard model on a honeycomb lattice may be simulated in an optical lattice of cold atoms. In Ref. 32, it is proposed that the (spinless) Haldane model on a honeycomb optical lattice can be realized in cold atoms. When two-component fermions with repulsive interaction are put into such an optical lattice, one can get an effective topological Hubbard model. It is easy to change the potential barrier by varying the laser intensities to tune the Hamiltonian parameters, including the hopping strength (t term), the staggered potential (ε term), and the particle interaction (U term).

ACKNOWLEDGMENTS

This work is supported by NFSC Grant No. 10874017, 11174035 and the National Basic Research Program of China (973 Program) under grants No. 2011CB921803, No. 2012CB921704, and No. 2011cba00102.

APPENDIX A: THEORY OF SPIN FLUCTUATIONS TO OBTAIN THE O(3) NONLINEAR σ MODEL

The Hamiltonian of the topological Hubbard model on a honeycomb lattice is given by

$$\begin{aligned} H = &-t\sum_{\langle i,j\rangle,\sigma}(\hat{c}^{\dagger}_{i\sigma}\hat{c}_{j\sigma}+\text{H.c.})-t'\sum_{\langle\langle i,j\rangle\rangle,\sigma}e^{i\phi_{ij}}\hat{c}^{\dagger}_{i\sigma}\hat{c}_{j\sigma}\\ &+U\sum_{i}\hat{n}_{i\uparrow}\hat{n}_{i\downarrow}-\mu\sum_{i,\sigma}\hat{c}^{\dagger}_{i\sigma}\hat{c}_{i\sigma}\\ &+\varepsilon\sum_{i\in A,\sigma}\hat{c}^{\dagger}_{i\sigma}\hat{c}_{i\sigma}-\varepsilon\sum_{i\in B,\sigma}\hat{c}^{\dagger}_{i\sigma}\hat{c}_{i\sigma}. \end{aligned} \tag{A1}$$

t and t' are the nearest-neighbor and the next-nearest-neighbor hoppings, respectively. We introduce a complex phase ϕ_{ij} ($|\phi_{ij}|=\frac{\pi}{2}$) to the next-nearest-neighbor hopping, of which the positive phase is set to be clockwise. U is the on-site Coulomb repulsion. σ are the spin indices representing spin-up ($\sigma=\uparrow$) and spin-down ($\sigma=\downarrow$) for electrons, and ε denotes an on-site staggered energy and is set to be $0.15t$.

For free fermions (the on-site Coulomb repulsion U is zero), the spectrum

$$E_{\mathbf{k}}=\sqrt{|\xi_k|^2+(\xi'_k+\varepsilon)^2}, \tag{A2}$$

where

$$|\xi_{\mathbf{k}}|=t\sqrt{3+2\cos(\sqrt{3}k_y)+4\cos(3k_x/2)\cos(\sqrt{3}k_y/2)}$$

and

$$\xi'_k=2t'\sum_i\sin(\mathbf{k}\cdot\mathbf{b}_i), \tag{A3}$$

where $\mathbf{b}_i$ denotes the next-nearest vectors. According to this spectrum $E_{\mathbf{k}}$, we can see that there are energy gaps Δ_{f1}, Δ_{f2} near points $\mathbf{k}_1=-\frac{2\pi}{3}(1,1/\sqrt{3})$ and $\mathbf{k}_2=\frac{2\pi}{3}(1,\ 1/\sqrt{3})$ as $\Delta_{f1}=|2\varepsilon-6\sqrt{3}t'|$ and $\Delta_{f2}=2\varepsilon+6\sqrt{3}t'$, respectively. There are two phases separated by the phase boundary $2\varepsilon=6\sqrt{3}t'$, namely the quantum anomalous Hall (QAH) state and the normal band insulator (BI) state with trivial topological properties.

Because the Hubbard model on bipartite lattices is unstable against antiferromagnetic instability, at half-filling the ground state may be an insulator with AF-SDW order with increasing interacting strength. Such AF-SDW order is described by the following mean-field order parameter: $\langle(-1)^i\hat{c}^{\dagger}_i\sigma^z\hat{c}_i\rangle=M$. Here M is the staggered magnetization. In the mean-field theory, the Hamiltonian of the topological Hubbard model is obtained as

$$H_{\text{MF}}=H-\sum_i(-1)^i\Delta_M\hat{c}^{\dagger}_i\sigma_z\hat{c}_i, \tag{A4}$$

where $\Delta_M=\frac{UM}{2}$. Then in momentum space we get

$$H=\sum_k c^{\dagger}_k h_k c_k, \tag{A5}$$

where $c^{\dagger}_k=(c^{\dagger}_{k,A\uparrow},c^{\dagger}_{k,A\downarrow},c^{\dagger}_{k,B\uparrow},c^{\dagger}_{k,B\downarrow})$ and

$$h_k=\begin{pmatrix}\xi_{\mathbf{k}'}+\frac{UM}{2}\sigma_z+\varepsilon & \xi_{\mathbf{k}}\\ (\xi_{\mathbf{k}})^* & -\xi_{\mathbf{k}'}-\frac{UM}{2}\sigma_z-\varepsilon\end{pmatrix}.$$

After diagonalization, we can obtain the quasiparticle spectra,

$$E_{\mathbf{k}_1}=\pm\sqrt{(\xi'_k+\Delta_M+\varepsilon)^2+|\xi_k|^2} \tag{A6}$$

and

$$E_{\mathbf{k}_2} = \pm\sqrt{(\xi'_k - \Delta_M + \varepsilon)^2 + |\xi_k|^2}. \tag{A7}$$

By minimizing the ground state's energy, the self-consistent equation in the reduced BZ is reduced to

$$1 = \frac{1}{N_s M}\sum_{\mathbf{k}\in \mathrm{BZ}}\left[\frac{\xi'_{\mathbf{k}} + \Delta_M + \varepsilon}{2E_{\mathbf{k}_1}} - \frac{\xi'_{\mathbf{k}} - \Delta_M + \varepsilon}{2E_{\mathbf{k}_2}}\right], \tag{A8}$$

where N_s is the number of unit cells. The phase diagram has been obtained in Ref. 15. There are a total of five phases: the NI state, the QAH state, the A-TSDW state, the B-TSDW state, and the trivial AF-SDW state. They are separated by two types of phase transitions: (i) the magnetic phase transition [denoted by $(U/t)_M$] between a magnetic order state with $M \neq 0$ and a nonmagnetic state with $M = 0$, and (ii) the topological quantum phase transition [denoted by $(\frac{U}{t})_{c1}$ or $(\frac{U}{t})_{c2}$] that is characterized by the condition of zero fermion energy gaps, $\Delta_{f1} = -6\sqrt{3}t' + 2\varepsilon + UM = 0$ or $\Delta_{f2} = 6\sqrt{3}t' + 2\varepsilon - UM = 0$.

We deal with the spin fluctuations by using the path-integral formulation of electrons with spin rotation symmetry. The interaction term can be handled by using the SU(2) invariant Hubbard-Stratonovich decomposition in the arbitrary on-site unit vector $\mathbf{\Omega}_i$,

$$\hat{n}_{i\uparrow}\hat{n}_{i\downarrow} = \frac{(\hat{c}_i^\dagger \hat{c}_i)^2}{4} - \frac{1}{4}[\mathbf{\Omega}_i \cdot \hat{c}_i^\dagger \boldsymbol{\sigma} \hat{c}_i]^2. \tag{A9}$$

Here $\boldsymbol{\sigma} = (\sigma_x, \sigma_y, \sigma_z)$ are the Pauli matrices. By replacing the electronic operators $\hat{c}_i^\dagger$ and $\hat{c}_j$ by Grassmann variables c_i^* and c_j, the effective Lagrangian of the 2D generalized Hubbard model at half-filling is obtained:

$$\begin{aligned}\mathcal{L}_{\mathrm{eff}} = &\sum_{i,\sigma} c^*_{i\sigma}\partial_\tau c_{i,\sigma} - t\sum_{\langle i,j\rangle,\sigma}(c^*_{i\sigma}c_{j\sigma} + \mathrm{H.c.})\\ &- t'\sum_{\langle\langle i,j\rangle\rangle,\sigma} e^{i\phi_{ij}} c^*_{i\sigma}c_{j\sigma} - \Delta_M\sum_{i,\sigma} c^*_{i,\sigma}\mathbf{\Omega}_i\cdot\boldsymbol{\sigma}c_{i,\sigma}\\ &+ \varepsilon\sum_{i\in A,\sigma} c^*_{i\sigma}c_{i\sigma} - \varepsilon\sum_{i\in B,\sigma} c^*_{i\sigma}c_{i\sigma}.\end{aligned} \tag{A10}$$

To describe the spin fluctuations, we use Haldane's mapping:

$$\mathbf{\Omega}_i = (-1)^i \mathbf{n}_i\sqrt{1-\mathbf{L}_i^2} + \mathbf{L}_i, \tag{A11}$$

where $\mathbf{n}_i = (n_i^x, n_i^y, n_i^z)$ is the Néel vector that corresponds to the long-wavelength part of $\mathbf{\Omega}_i$ with a restriction $\mathbf{n}_i^2 = 1$. $\mathbf{L}_i$ is the transverse canting field that corresponds to the short-wavelength parts of $\mathbf{\Omega}_i$ with a restriction $\mathbf{L}_i \cdot \mathbf{n}_i = \mathbf{0}$. We then rotate $\mathbf{\Omega}_i$ to the $\hat{\mathbf{z}}$ axis for the spin indices of the electrons at i site:

$$\psi_i = U_i^\dagger c_i, \tag{A12}$$

$$U_i^\dagger \mathbf{n}_i \cdot \boldsymbol{\sigma} U_i = \boldsymbol{\sigma}_z, \tag{A13}$$

$$U_i^\dagger \mathbf{L}_i \cdot \boldsymbol{\sigma} U_i = \mathbf{l}_i \cdot \boldsymbol{\sigma}, \tag{A14}$$

where $U_i \in \mathrm{SU(2)/U(1)}$.

One then can derive the following effective Lagrangian after such spin transformation:

$$\begin{aligned}\mathcal{L}_{\mathrm{eff}} = &\sum_{i,\sigma}\psi^*_{i,\sigma}\partial_\tau\psi_{i,\sigma} + \sum_{i,\sigma}\psi^*_{i,\sigma}a_0(i)\psi_{i,\sigma}\\ &- t\sum_{\langle i,j\rangle,\sigma}(\psi^*_{i,\sigma}e^{ia_{ij}}\psi_{j,\sigma} + \mathrm{H.c.}) - t'\sum_{\langle\langle i,j\rangle\rangle,\sigma} e^{i\phi_{ij}}\psi^*_{i,\sigma}e^{ia_{ij}}\psi_{j,\sigma}\\ &+ \varepsilon\sum_{i\in A,\sigma}\psi^*_{i,\sigma}e^{ia_{ii}}\psi_{i,\sigma} - \varepsilon\sum_{i\in B,\sigma}\psi^*_{i,\sigma}e^{ia_{ii}}\psi_{i,\sigma}\\ &- \Delta_M\sum_{i,\sigma}\psi^*_{i,\sigma}\left[(-1)^i\boldsymbol{\sigma}_z\sqrt{1-\mathbf{l}_i^2} + \mathbf{l}_i\cdot\boldsymbol{\sigma}\right]\psi_{i,\sigma},\end{aligned} \tag{A15}$$

where the auxiliary gauge fields $a_{ij} = a_{ij,1}\sigma_x + a_{ij,2}\sigma_y$ and $a_0(i) = a_{0,1}(i)\sigma_x + a_{0,2}(i)\sigma_y$ are defined as

$$e^{ia_{ij}} = U_i^\dagger U_j,\ a_0(i) = U_i^\dagger\partial_\tau U_i. \tag{A16}$$

In terms of the mean-field result $M = (-1)^i\langle\psi_i^*\boldsymbol{\sigma}_z\psi_i\rangle$ as well as the approximations,

$$\sqrt{1-\mathbf{l}_i^2} \simeq 1 - \frac{\mathbf{l}_i^2}{2},\quad e^{ia_{ij}} \simeq 1 + ia_{ij},$$

we obtain the effective Hamiltonian as

$$\begin{aligned}\mathcal{L}_{\mathrm{eff}} \simeq &\sum_{i,\sigma}\psi^*_{i,\sigma}\partial_\tau\psi_{i,\sigma} + \sum_{i,\sigma}\psi^*_{i,\sigma}[a_0(i) - \Delta\mathbf{l}_i\cdot\boldsymbol{\sigma}]\psi_{i,\sigma}\\ &- \Delta_M\sum_{i,\sigma}(-1)^i\psi^*_{i,\sigma}\boldsymbol{\sigma}_z\psi_{i,\sigma} - t\sum_{\langle i,j\rangle,\sigma}\psi^*_{i,\sigma}(1+ia_{ij})\psi_{j,\sigma}\\ &- t'\sum_{\langle\langle i,j\rangle\rangle,\sigma} e^{i\phi_{ij}}\psi^*_{i,\sigma}(1+ia_{ij})\psi_{j,\sigma} + \Delta M\sum_{i,\sigma}\frac{\mathbf{l}_i^2}{2}\\ &+ \varepsilon\sum_{i\in A,\sigma}\psi^*_{i,\sigma}(1+ia_{ii})\psi_{i,\sigma} - \varepsilon\sum_{i\in B,\sigma}\psi^*_{i,\sigma}(1+ia_{ii})\psi_{i,\sigma}.\end{aligned} \tag{A17}$$

By integrating out the fermion fields ψ_i^* and ψ_i, the effective action with the quadric terms of $[a_0(i) - \Delta\boldsymbol{\sigma}\cdot l_i]$ and a_{ij} becomes

$$\begin{aligned}\mathcal{S}_{\mathrm{eff}} = \frac{1}{2}\int_0^\beta d\tau\sum_i\Big[&-4\varsigma[a_0(i) - \Delta_M\boldsymbol{\sigma}\cdot l_i]^2\\ &+ 4\rho_s a_{ij}^2 + \frac{2\Delta_M^2}{U}\mathbf{l}_i^2\Big].\end{aligned} \tag{A18}$$

To give ρ_s and ς for calculation in detail, we choose U_i to be

$$U_i = \begin{pmatrix} z^*_{i\uparrow} & z^*_{i\downarrow}\\ -z_{i\downarrow} & z_{i\uparrow}\end{pmatrix}, \tag{A19}$$

where $\mathbf{n}_i = \bar{\mathbf{z}}_i\boldsymbol{\sigma}\mathbf{z}_i, \mathbf{z}_i = (z_{i\uparrow}, z_{i\downarrow})^T, \bar{\mathbf{z}}_i\mathbf{z}_i = \mathbf{1}$, and the spin fluctuations around $\mathbf{n}_i = \hat{\mathbf{z}}_i$ are

$$\mathbf{n}_i = \hat{\mathbf{z}}_i + \mathrm{Re}(\phi_i)\hat{\mathbf{x}} + \mathrm{Im}(\phi_i)\hat{\mathbf{y}}, \tag{A20}$$

$$\mathbf{z}_i = \begin{pmatrix} 1 - |\phi_i|^2/8\\ \phi_i/2\end{pmatrix} + O\left(\phi_i^3\right). \tag{A21}$$

Then the quantities $U_i^\dagger U_j$ and $U_i^\dagger \partial_\tau U_i$ can be expanded in powers of $\phi_i - \phi_j$ and $\partial_\tau \phi_i$,

$$U_i^\dagger U_j = e^{-i\frac{\phi_i-\phi_j}{2}\sigma_y}, \tag{A22}$$

$$U_i^\dagger \partial_\tau U_i = \begin{pmatrix} 0 & \frac{1}{2}\partial_\tau\phi_i \\ -\frac{1}{2}\partial_\tau\phi_i & 0 \end{pmatrix}. \tag{A23}$$

According to Eq. (A16), the gauge fields a_{ij} and $a_0(i)$ are given as

$$a_{ij} = -\frac{1}{2}(\phi_i - \phi_j)\boldsymbol{\sigma}_y, \tag{A24}$$

$$a_0(i) = \frac{i}{2}\partial_\tau\phi_i\boldsymbol{\sigma}_y. \tag{A25}$$

Supposing a_{ij} and $a_0(i)$ to be a constant in space and denoting $\boldsymbol{\partial}_i\phi_i = \mathbf{a}$ and $\partial_\tau\phi_i = iB_y$, we have

$$a_{ij} = -\tfrac{1}{2}\mathbf{a}\cdot(\mathbf{i}-\mathbf{j})\sigma_y, \tag{A26}$$

$$a_0(i) = -\tfrac{1}{2}B_y\sigma_y. \tag{A27}$$

The energy of the Hamiltonian of Eq. (A18) becomes

$$E(B_y,\mathbf{a}) = -\tfrac{1}{2}\zeta B_y^2 + \tfrac{1}{2}\rho_s\mathbf{a}^2. \tag{A28}$$

Then one could get ζ and ρ_s from the following equations by calculating the partial derivative of the energy:

$$\zeta = -\frac{1}{N}\frac{\partial^2 E_0(B_y)}{\partial B_y^2}\bigg|_{B_y=0}, \tag{A29}$$

$$\rho_s = \frac{1}{N}\frac{\partial^2 E_0(\mathbf{a})}{\partial \mathbf{a}^2}\bigg|_{\mathbf{a}=\mathbf{0}}. \tag{A30}$$

Here $E_0(B_y)$ and $E_0(\mathbf{a})$ are the energy of the lower Hubbard band,

$$E_0(B_y) = \sum_{\mathbf{k}}\left(E^\zeta_{+,\mathbf{k}} + E^\zeta_{-,\mathbf{k}}\right), \tag{A31}$$

$$E_0(\mathbf{a}) = \sum_{\mathbf{k}}\left(E^\rho_{+,\mathbf{k}} + E^\rho_{-,\mathbf{k}}\right), \tag{A32}$$

where $E^\zeta_{+,\mathbf{k}}$, $E^\zeta_{-,\mathbf{k}}$ and $E^\rho_{+,\mathbf{k}}$, $E^\rho_{-,\mathbf{k}}$ are the energies of the following Hamiltonian $\mathcal{H}^\zeta$ and $\mathcal{H}^\rho$:

$$\begin{aligned}\mathcal{H}^\zeta = &-t\sum_{\langle i,j\rangle,\sigma}(\psi^*_{i,\sigma}\psi_{j,\sigma} + \text{H.c.}) - t'\sum_{\langle\langle i,j\rangle\rangle,\sigma} e^{i\phi_{ij}}\psi^*_{i,\sigma}\psi_{j,\sigma} + \varepsilon\sum_{i\in A,\sigma}\psi^*_{i,\sigma}\psi_{i,\sigma} - \varepsilon\sum_{i\in B,\sigma}\psi^*_{i,\sigma}\psi_{i,\sigma} \\ &+ \sum_{i,\sigma}\psi^*_{i,\sigma}a_0(i)\psi_{i,\sigma} - \Delta_M\sum_{i,\sigma}(-1)^i\psi^*_{i,\sigma}\boldsymbol{\sigma}_z\psi_{i,\sigma},\end{aligned} \tag{A33}$$

$$\begin{aligned}\mathcal{H}^\rho = &-t\sum_{\langle i,j\rangle,\sigma}\psi^*_{i,\sigma}e^{ia_{ij}}\psi_{j,\sigma} - t'\sum_{\langle\langle i,j\rangle\rangle,\sigma} e^{i\phi_{ij}}\psi^*_{i,\sigma}e^{ia_{ij}}\psi_{j,\sigma} + \varepsilon\sum_{i\in A,\sigma}\psi^*_{i,\sigma}e^{ia_{ii}}\psi_{i,\sigma} - \varepsilon\sum_{i\in B,\sigma}\psi^*_{i,\sigma}e^{ia_{ii}}\psi_{i,\sigma} \\ &- \Delta_M\sum_{i,\sigma}(-1)^i\psi^*_{i,\sigma}\boldsymbol{\sigma}_z\psi_{i,\sigma}.\end{aligned} \tag{A34}$$

Using the Fourier transformation for $\mathcal{H}^\zeta$, we have the spectrum of the lower band of $\mathcal{H}^\zeta$:

$$E^\zeta_{\pm,\mathbf{k}} = -\frac{1}{2}\sqrt{4|\xi_k|^2 + 2a^2 + B_y^2 + 2d^2 \pm 2\sqrt{a^4 + B_y^2a^2 - 2a^2d^2 + B_y^2d^2 + 4B_y^2|\xi_k|^2 + d^4 + 2adB_y^2}}, \tag{A35}$$

where $a = \xi_{k'} + \frac{UM}{2} + \varepsilon$ and $d = \xi_{k'} - \frac{UM}{2} + \varepsilon$.

Using $\varsigma = -\frac{1}{N}\frac{\partial^2 E_0(B_y)}{\partial B_y^2}|_{B_y=0}$ and $E_0(B_y) = \sum_{\mathbf{k}}(E^\varsigma_{+,\mathbf{k}} + E^\varsigma_{-,\mathbf{k}})$, we can obtain ς as

$$\varsigma = \frac{-1}{N_s}\sum_{\mathbf{k}}\frac{1}{8\sqrt{2}}\left(\frac{-2 + \frac{2[4|\xi_k|^2+(a+d)^2]}{\sqrt{(a^2-d^2)^2}}}{\sqrt{a^2 + 2|\xi_k|^2 + d^2 - \sqrt{(d^2-a^2)^2}}} - \frac{2 + \frac{2[4|\xi_k|^2+(a+d)^2]}{\sqrt{(a^2-d^2)^2}}}{\sqrt{a^2 + 2|\xi_k|^2 + d^2 + \sqrt{(d^2-a^2)^2}}}\right). \tag{A36}$$

Similarly, using the Fourier transformation for $\mathcal{H}^\rho$, we have the spectrum of the lower band of $\mathcal{H}^\rho$:

$$E^\rho_{\pm,\mathbf{k}} = -\tfrac{1}{2}[4|\psi|^2 + 2G^2 - 4B^2 + 4|\varphi|^2 + 2A^2 \pm 2(4|\psi|^2G^2 - 8AG|\psi|^2 + 8AB\psi^*\varphi \tag{A37}$$

$$\begin{aligned}&- 8AB\varphi^*\psi + 8B\psi^*\varphi G - 8\varphi^*B\psi G - 2A^2G^2 - 4(\varphi^*\psi - \psi^*\varphi)^2 \\ &- 8AGB^2 - 4G^2B^2 + G^4 - 4B^2A^2 + A^4 + 4A^2|\psi|^2)^{\frac{1}{2}}]^{\frac{1}{2}},\end{aligned} \tag{A38}$$

where

$$A = 2t'\sum_i\cos\left(\frac{1}{2}\mathbf{a}\cdot\mathbf{b}_i\right)\sin(\mathbf{k}\cdot\mathbf{b}_i) + \varepsilon + \frac{UM}{2}, \quad G = 2t'\sum_i\cos\left(\frac{1}{2}\mathbf{a}\cdot\mathbf{b}_i\right)\sin(\mathbf{k}\cdot\mathbf{b}_i) + \varepsilon - \frac{UM}{2},$$

$$B = -2it'\sum_i\sin\left(\frac{1}{2}\mathbf{a}\cdot\mathbf{b}_i\right)\cos(\mathbf{k}\cdot\mathbf{b}_i), \quad \varphi = -t\sum_\delta e^{i\mathbf{k}\cdot\delta}\cos\left(\frac{1}{2}\mathbf{a}\cdot\delta\right), \quad \psi = -t\sum_\delta e^{i\mathbf{k}\cdot\delta}\sin\left(\frac{1}{2}\mathbf{a}\cdot\delta\right).$$

Using $\rho_s = \frac{1}{N}\frac{\partial^2 E_0(\mathbf{a})}{\partial \mathbf{a}^2}|_{\mathbf{a}=0}$ and $E_0(\mathbf{a}) = \sum_{\mathbf{k}} (E^{\rho}_{+,\mathbf{k}} + E^{\rho}_{-,\mathbf{k}})$, we can get $\rho_s = \rho_{s1} + \rho_{s2}$, where

$$\rho_{s1} = \frac{-1}{N_s}\sum_{\mathbf{k}}\Bigg\{ -9t^2\cos\left(\frac{3k_x}{2}\right)\cos\left(\frac{\sqrt{3}k_y}{2}\right) - 36t'^2[-1+\cos(\sqrt{3}k_y)]\sin^2\left(\frac{3k_x}{2}\right) - 9t'(P+Q)\cos\left(\frac{3k_x}{2}\right)\sin\left(\frac{\sqrt{3}k_y}{2}\right)$$
$$+\Bigg[3\{t^2[(P-Q)^2+6t^2] + 18t'^2(P+Q)^2 - 18[t^4 + t'^2(P+Q)^2]\cos(3k_x)\} - 4t^2(P-Q)^2\cos\left(\frac{3k_x}{2}\right)\cos\left(\frac{\sqrt{3}k_y}{2}\right)$$
$$+\{t^2[(P-Q)^2+18t^2] - 18t'^2(P+Q)^2 + 18[t'^2(P+Q)^2 - t^4]\cos(3k_x)\}\cos(\sqrt{3}k_y) - 9t'(P-Q)^2(P+Q)\cos\left(\frac{3k_x}{2}\right)$$
$$\times\sin\left(\frac{\sqrt{3}k_y}{2}\right) + 72t^2t'(P+Q)\sin^2\left(\frac{3k_x}{2}\right)\sin(\sqrt{3}k_y)\Bigg]\Big/\sqrt{(P^2-Q^2)^2}\Bigg\}\Big/8\sqrt{2}\sqrt{P^2+Q^2+2|\xi_k|^2+\sqrt{(P^2-Q^2)^2}} \tag{A39}$$

and

$$\rho_{s2} = \frac{-1}{N_s}\sum_{\mathbf{k}}\Bigg\{ -9t^2\cos\left(\frac{3k_x}{2}\right)\cos\left(\frac{\sqrt{3}k_y}{2}\right) - 36t'^2[-1+\cos(\sqrt{3}k_y)]\sin^2\left(\frac{3k_x}{2}\right) - 9t'(P+Q)\cos\left(\frac{3k_x}{2}\right)\sin\left(\frac{\sqrt{3}k_y}{2}\right)$$
$$-\Bigg[3\{t^2[(P-Q)^2+6t^2] + 18t'^2(P+Q)^2 - 18[t^4 + t'^2(P+Q)^2]\cos(3k_x)\} - 4t^2(P-Q)^2\cos\left(\frac{3k_x}{2}\right)\cos\left(\frac{\sqrt{3}k_y}{2}\right)$$
$$+\{t^2[(P-Q)^2+18t^2] - 18t'^2(P+Q)^2 + 18[t'^2(P+Q)^2 - t^4]\cos(3k_x)\}\cos(\sqrt{3}k_y) - 9t'(P-Q)^2(P+Q)\cos\left(\frac{3k_x}{2}\right)$$
$$\times\sin\left(\frac{\sqrt{3}k_y}{2}\right) + 72t^2t'(P+Q)\sin^2\left(\frac{3k_x}{2}\right)\sin(\sqrt{3}k_y)\Bigg]\Big/\sqrt{(P^2-Q^2)^2}\Bigg\}\Big/8\sqrt{2}\sqrt{P^2+Q^2+2|\xi_k|^2-\sqrt{(P^2-Q^2)^2}}, \tag{A40}$$

where $P = \xi_{k'} - \frac{UM}{2} + \varepsilon$ and $Q = \xi_{k'} + \frac{UM}{2} + \varepsilon$.

In addition, we study the continuum theory of the effective action. In the continuum limit, we denote $\mathbf{n}_i, \mathbf{l}_i, ia_{ij} \simeq U_i^{\dagger}U_j - 1$, and $a_0(i) = U_i^{\dagger}\partial_\tau U_i$ by $\mathbf{n}(x,y)$, $\mathbf{l}(x,y)$, $U^{\dagger}\partial_x U$ (or $U^{\dagger}\partial_y U$), and $U^{\dagger}\partial_\tau U$, respectively. From the relations between $U^{\dagger}\partial_\mu U$ and $\partial_\mu \mathbf{n}$,

$$a_\tau^2 = a_{\tau,1}^2 + a_{\tau,2}^2 = -\frac{1}{4}(\partial_\tau \mathbf{n})^2,\ \tau = 0, \tag{A41}$$

$$a_\mu^2 = a_{\mu,1}^2 + a_{\mu,2}^2 = \frac{1}{4}(\partial_\mu \mathbf{n})^2,\ \mu = x,y, \tag{A42}$$

$$\mathbf{a}_0\cdot\mathbf{l} = -\frac{i}{2}(\mathbf{n}\times\partial_\tau\mathbf{n})\cdot\mathbf{l}, \tag{A43}$$

the continuum formulation of the action becomes

$$\mathcal{S}_{\text{eff}} = \frac{1}{2}\int_0^\beta d\tau\int d^2\mathbf{r}\Big[\varsigma(\partial_\tau\mathbf{n})^2 + \rho_s(\nabla\cdot\mathbf{n})^2 - 4i\Delta_M\varsigma(\mathbf{n}\times\partial_\tau\mathbf{n})\cdot\mathbf{l} + \left(\frac{2\Delta_M^2}{U} - 4\Delta_M^2\varsigma\right)\mathbf{l}^2\Big], \tag{A44}$$

where the vector $\mathbf{a}_0$ is defined as $\mathbf{a}_0 = (a_{0,1}, a_{0,2}, 0)$.

Finally, we integrate the transverse canting field $\mathbf{l}$ and obtain the effective NLσM as

$$\mathcal{S}_{\text{eff}} = \frac{1}{2g}\int_0^\beta d\tau\int d^2r\Big[\frac{1}{c}(\partial_\tau\mathbf{n})^2 + c(\nabla\cdot\mathbf{n})^2\Big] \tag{A45}$$

with a constraint $\mathbf{n}^2 = 1$. The coupling constant g and spin wave velocity c are defined as $g = \sqrt{\frac{1}{\rho_s\chi^{\perp}}}$, $c^2 = \frac{\rho_s}{\chi^{\perp}}$, and $\chi^{\perp}$ is the transverse spin susceptibility,

$$\chi^{\perp} = [\varsigma^{-1} - 2U]^{-1}. \tag{A46}$$

In addition, we need to determine another important parameter—the cutoff Λ. On the one hand, the effective NLσM is valid within the energy scale of the electrons' gap, ΔE. On the other hand, the lattice constant is a natural cutoff. Thus the cutoff is defined as the following equation:

$$\Lambda = \min\left(1, \frac{\Delta E}{c}\right). \tag{A47}$$

APPENDIX B: INDUCED CSH TERMS

In this Appendix, we will derive the low-energy effective theory of (T-)SDW states by considering quantum fluctuations of effective spin moments based on a formulation by keeping spin rotation symmetry, $\sigma_z \to \mathbf{n}\cdot\boldsymbol{\sigma}$, where $\mathbf{n}$ is the SDW order parameter, $\langle \hat{c}_i^\dagger \boldsymbol{\sigma} \hat{c}_i\rangle = M\mathbf{n}$.

On a honeycomb lattice, after dividing the lattice into two sublattices, A and B, the dispersion can be obtained from Eq. (2). In the continuum limit, the Dirac-like effective Lagrangian describes the low-energy fermionic modes near two points, $\mathbf{k}_1 = -\frac{2\pi}{3}(1,\frac{1}{\sqrt{3}})$ and $\mathbf{k}_2 = \frac{2\pi}{3}(1,\frac{1}{\sqrt{3}})$, as

$$\mathcal{L}_f = \sum_a [i\bar{\psi}_a\gamma_\mu(\partial_\mu - iA_\mu)\psi_a + m_a\bar{\psi}_a\psi_a - \delta\Delta_M\bar{\psi}_a\boldsymbol{\sigma}\cdot\mathbf{n}\psi_a], \tag{B1}$$

which describes low-energy charged fermionic modes $a=1$ near $\mathbf{k}_1$,

$$\bar{\psi}_1 = \psi_1^\dagger\gamma_0 = (\bar{\psi}_{\uparrow 1A},\quad \bar{\psi}_{\uparrow 1B},\quad \bar{\psi}_{\downarrow 1A},\quad \bar{\psi}_{\downarrow 1B}) \tag{B2}$$

and $a=2$ near $\mathbf{k}_2$,

$$\bar{\psi}_2 = \psi_2^\dagger\gamma_0 = (\bar{\psi}_{\uparrow 2B},\ \bar{\psi}_{\uparrow 2A},\ \bar{\psi}_{\downarrow 2B},\ \bar{\psi}_{\downarrow 2A}). \tag{B3}$$

The masses of two-flavor fermions are

$$m_1 = \varepsilon - 3\sqrt{3}t' \tag{B4}$$

and

$$m_2 = \varepsilon + 3\sqrt{3}t'. \tag{B5}$$

γ_μ is defined as $\gamma_0 = \sigma_0\otimes\tau_z, \gamma_1 = \sigma_0\otimes\tau_y,\ \gamma_2 = \sigma_0\otimes\tau_x$ with $\sigma_0 = \left(\begin{smallmatrix}1 & 0\\ 0 & 1\end{smallmatrix}\right)$. τ_x, τ_y, τ_z are Pauli matrices. $\delta = 1$ for $a=1$ and $\delta=-1$ for $a=2$. We have set the Fermi velocity to be unit $v_F = 1$.

In the CP^1 representation, we may rewrite the effective Lagrangian of fermions in Eq. (B1) as

$$\mathcal{L}_f = \sum_a \bar{\psi}'_a(i\gamma_\mu\partial_\mu + \gamma_\mu A_\mu - \gamma_\mu\sigma_3 a_\mu + m_a - \delta\Delta_M\sigma_3)\psi'_a \tag{B6}$$

with

$$\psi'_a(r,\tau) = U^\dagger(r,\tau)\psi_a(r,\tau),$$

where $U(r,\tau)$ is a local and time-dependent spin SU(2) transformation defined by

$$U^\dagger(r,\tau)\mathbf{n}\cdot\sigma U(r,\tau) = \sigma_3$$

and a_μ is introduced as an assistant gauge field as

$$i\sigma_3 a_\mu \equiv U^\dagger(r,\tau)\partial_\mu U(r,\tau).$$

An important property of the model in Eq. (B6) is the current anomaly. The vacuum expectation value of the fermionic current,

$$J^\mu_{a,\sigma} = i\langle\bar{\psi}_{a,\sigma}\gamma^\mu\psi_{a,\sigma}\rangle, \tag{B7}$$

can be defined by

$$J^\mu_{a,\sigma} = i\{\gamma^\mu[(i\hat{D}+im_{a,\sigma})^\dagger(i\hat{D}+im_{a,\sigma})]^{-1}(i\hat{D}+im_{a,\sigma})^\dagger\}, \tag{B8}$$

where

$$\hat{D} = \gamma_\mu(\partial_\mu - iA_\mu + i\sigma a_\mu) \tag{B9}$$

and the mass terms are $m_{a,\sigma} = m_a - \delta\Delta_M\sigma$. The topological current $J^\mu_{a,\sigma}$ is obtained to be

$$J^\mu_{a,\sigma} = \frac{1}{2}\frac{1}{4\pi}\frac{m_{a,\sigma}}{|m_{a,\sigma}|}\epsilon^{\mu\nu\lambda}(\partial_\nu A_\lambda - \sigma\partial_\nu a_\lambda). \tag{B10}$$

Then we derive the CSH terms as[40–42]

$$\mathcal{L}_{\rm CSH} = -i\sum_{a,\sigma}(A_\mu - \sigma a_\mu)J^\mu_{a,\sigma}. \tag{B11}$$

To make an explicit description of SDWs, we introduce the $\mathcal{K}$-matrix formulation that has been used to characterize FQH fluids successfully.[24] Now the CSH term is written as

$$\mathcal{L}_{\rm CSH} = -i\sum_{I,J}\frac{\mathcal{K}_{IJ}}{4\pi}\varepsilon^{\mu\nu\lambda}a^I_\mu\partial_\nu a^J_\lambda, \tag{B12}$$

where $\mathcal{K}$ is a 2×2 matrix, $a^{I=1}_\mu = A_\mu$, and $a^{I=2}_\mu = a_\mu$. The "charges" of A_μ and a_μ are defined by q and q_s, respectively.

Thus for different SDW orders with the same order parameter M, we have different $\mathcal{K}$ matrices: for $m_1, m_2 > \Delta_M$,

$$\mathcal{K} = \begin{pmatrix}2 & 0\\ 0 & 2\end{pmatrix}, \tag{B13}$$

for $m_2 > \Delta_M > m_1$,

$$\mathcal{K} = \begin{pmatrix}1 & 1\\ 1 & 1\end{pmatrix}, \tag{B14}$$

for $m_1, m_2 < \Delta_M$,

$$\mathcal{K} = 0. \tag{B15}$$

These results are consistent with those of Ref. 15.

*Author to whom all correspondence should be addressed: spkou@bnu.edu.cn

[1] P. W. Anderson, Science **235**, 1196 (1987).
[2] P. Fazekas and P. W. Anderson, Philos. Mag. **30**, 432 (1974).
[3] X. G. Wen, *Quantum Field Theory of Many-Body Systems* (Oxford University Press, Oxford, 2004).
[4] X. G. Wen, Phys. Rev. B **65**, 165113 (2002).
[5] S. S. Lee and P. A. Lee, Phys. Rev. Lett. **95**, 036403 (2005).
[6] M. Hermele, Phys. Rev. B **76**, 035125 (2007).
[7] G. Y. Sun and S. P. Kou, Europhys. Lett. **87**, 67002 (2009).
[8] Z. Y. Meng, T. C. Lang, S. Wessel, F. F. Assaad, and A. Muramatsu, Nature (London) **464**, 847 (2010).
[9] G. Y. Sun and S. P. Kou, J. Phys.: Condens. Matter **23**, 045603 (2011).
[10] F. Wang, Phys. Rev. B **82**, 024419 (2010).

[11] Y.-M. Lu and Y. Ran, Phys. Rev. B **84**, 024420 (2011); e-print arXiv:1007.3266.
[12] B. K. Clark, D. A. Abanin, and S. L. Sondhi, Phys. Rev. Lett. **107**, 087204 (2011).
[13] G. Wang, M. O. Goerbig, B. Gremaud, and C. Miniatura, Europhys. Lett. **95**, 47013 (2011).
[14] A. Vaezi and X.-G. Wen, e-print arXiv:1010.5744.
[15] J. He, Y. H. Zong, S. P. Kou, Y. Liang, and S. P. Feng, Phys. Rev. B **84**, 035127 (2011).
[16] F. D. M. Haldane, Phys. Rev. Lett. **61**, 2015 (1988).
[17] J. He, S. P. Kou, Y. Liang, and S. P. Feng, Phys. Rev. B **83**, 205116 (2011).
[18] F. D. M. Haldane, Phys. Lett. A **93**, 464 (1983).
[19] A. Auerbach, *Interacting Electrons and Quantum Magnetism* (Springer-Verlag, New York, 1994).
[20] N. Dupuis, Phys. Rev. B **65**, 245118 (2002).
[21] K. Borejsza and N. Dupuis, Europhys. Lett. **63**, 722 (2003); Phys. Rev. B **69**, 085119 (2004).
[22] H. J. Schulz, Phys. Rev. Lett. **65**, 2462 (1990); in *The Hubbard Model*, edited by D. Baeriswyl (Plenum, New York, 1995).
[23] Z. Y. Weng, C. S. Ting, and T. K. Lee, Phys. Rev. B **43**, 3790 (1991).
[24] B. Blok and X.-G. Wen, Phys. Rev. B **42**, 8133 (1990); **42**, 8145 (1990); X.-G. Wen and A. Zee, *ibid*. **46**, 2290 (1992).
[25] S. P. Kou, L. F. Liu, J. He, and Y. J. Wu, Eur. Phys. J. B **81**, 165 (2011).
[26] A. M. Polyakov, Nucl. Phys. B **120**, 429 (1977); *Gauge Fields and Strings* (Harwood Academic, London, 1987).
[27] A. Vaezi and X. G. Wen, e-print arXiv:1101.1662.
[28] X. G. Wen, F. Wilczek, and A. Zee, Phys. Rev. B **39**, 11413 (1989).
[29] X. G. Wen, Phys. Rev. B **40**, 7387 (1989); Int. J. Mod. Phys. B **2**, 239 (1990).
[30] B. I. Halperin, Phys. Rev. B **25**, 2185 (1982).
[31] A. A. Belavin and A. M. Polyakov, JETP Lett. **22**, 245 (1975).
[32] L. B. Shao, S. L. Zhu, L. Sheng, D. Y. Xing, and Z. D. Wang, Phys. Rev. Lett. **101**, 246810 (2008).
[33] D. C. Tsui, H. L. Stormer, and A. C. Gossard, Phys. Rev. Lett. **48**, 1559 (1982).
[34] R. B. Laughlin, Phys. Rev. Lett. **50**, 1395 (1983).
[35] N. Read, Phys. Rev. Lett. **65**, 1502 (1990).
[36] J. Fröhlich and T. Kerler, Nucl. Phys. B **354**, 369 (1991); J. Fröhlich and A. Zee, *ibid*. **364**, 517 (1991).
[37] M. R. Zirnbauer, J. Math. Phys. **37**, 4986 (1996); A. Altland and M. R. Zirnbauer, Phys. Rev. B **55**, 1142 (1997).
[38] A. Y. Kitaev, in *Periodic Table for Topological Insulators and Superconductors*, AIP Conf. Proc. No. 1134 (AIP, New York, 2009), p. 22.
[39] S. Ryu, A. P Schnyder, A. Furusaki, and A. W. W. Ludwig, New J. Phys. **12**, 065010 (2010).
[40] A. N. Redlich, Phys. Rev. Lett. **52**, 18 (1984); Phys. Rev. D **29**, 2366 (1984).
[41] K. Ishikawa and T. Matsuyama, Z. Phys. C **33**, 41 (1986); Nucl. Phys. B **280**, 523 (1987).
[42] A. J. Niemi and G. W. Semenoff, Phys. Rev. Lett. **51**, 2077 (1983).